Inclusion body myositis-like phenotype induced by transgenic overexpression of βAPP in skeletal muscle

Michael C. Sugarman*, Tritia R. Yamasaki*, Salvatore Oddo*, Julio C. Echegoyen*, M. Paul Murphy†, Todd E. Golde†, Mehrdad Jannatipour*, Malcolm A. Leissring*, and Frank M. LaFerla*‡

*Department of Neurobiology and Behavior, University of California, Irvine, CA 92697; and †Department of Neuroscience and Pharmacology, Mayo Clinic Jacksonville, Jacksonville, FL 32224

Edited by Laszlo Lorand, Northwestern University Medical School, Chicago, IL, and approved February 14, 2002 (received for review October 12, 2001)

Inclusion body myositis (IBM), the most common age-related muscle disease in the elderly population, is an incurable disorder leading to severe disability. Sporadic IBM has an unknown etiology, although affected muscle fibers are characterized by many of the pathobiochemical alterations traditionally associated with neurodegenerative brain disorders such as Alzheimer's disease. Accumulation of the amyloid-β peptide, which is derived from proteolysis of the larger amyloid-β precursor protein (βAPP), seems to be an early pathological event in Alzheimer's disease and also in IBM, where in the latter, it predominantly occurs intracellularly within affected myofibers. To elucidate the possible role of βAPP mismetabolism in the pathogenesis of IBM, transgenic mice were derived in which we selectively targeted βAPP overexpression to skeletal muscle by using the muscle creatine kinase promoter. Here we report that older (>10 months) transgenic mice exhibit intracellular immunoreactivity to βAPP and its proteolytic derivatives in skeletal muscle. In this transgenic model, selective overexpression of βAPP leads to the development of a subset of other histopathological and clinical features characteristic of IBM, including centric nuclei, inflammation, and deficiencies in motor performance. These results are consistent with a pathogenic role for βAPP mismetabolism in human IBM.

Brain and skeletal muscle are the only known tissues in humans marked by the pathological accumulation of the amyloid-β (Aβ) peptide. In brain, Aβ deposition is associated with several genetically related neurodegenerative disorders including Alzheimer's disease (AD), Down syndrome, and hereditary cerebral hemorrhage with amyloidosis–Dutch type (1). On the basis of genetic evidence, Aβ accumulation seems to be an early pathogenic event, although it remains to be determined whether Aβ directly leads to cell degeneration or whether cell degeneration is mediated by other downstream factors induced by it. In muscle, Aβ accumulation is associated with inclusion body myositis (IBM), the most common muscle disorder to afflict the elderly. IBM is the first human disorder marked by the pathological accumulation of this amyloidogenic peptide outside the central nervous system. Notably, Aβ and/or other Aβ-containing fragments produced by proteolysis of the amyloid-β precursor protein (βAPP) are not implicated in other myopathies, suggesting that βAPP mismetabolism is an integral component of the molecular pathogenesis of IBM.

Like AD, IBM is an age-related degenerative disorder with a slowly progressive clinical course for which no effective treatment is available. Clinically characterized by muscle weakness and atrophy involving both proximal and distal muscle groups (2–4), IBM was first recognized as its own disorder in the early 1970s (5); before that, it was often diagnosed as polymyositis (6). That Aβ-containing fragments are involved in the pathogenesis of IBM is somewhat surprising because no obvious genetic link exists to either the βAPP gene or to other AD-related genes such as apolipoprotein E (7, 8). Nevertheless, IBM and AD share many pathobiochemical features, including twisted intracellular tubulofilaments consisting of hyperphosphorylated tau (9) and the aberrant accumulation of other "dementia"-related proteins, including apoE, presenilin, prion protein, and α-synuclein (10–13). These data suggest that after an initial insult, a coordinated molecular cascade occurs, triggering the accumulation of these "dementia"-related proteins both in muscle and in brain. Along these lines, AD patients also contain slightly elevated levels of amyloidogenic $A\beta_{1-42}$ peptides in their muscle, but these elevated levels seem to be without pathological consequence, perhaps because of low steady-state levels (14). Curiously, it has been reported that myoglobin can also form amyloid fibrils, but whether this ability plays a role in muscle disease is not yet established (15).

One interesting distinction between IBM and AD involves the location of the Aβ deposits. Whereas the AD brain is characterized by accumulation of amyloid deposits in extracellular plaques, Aβ accumulates *intracellularly* in IBM (16). Although Aβ accumulates intraneuronally according to reports (17, 18), it has not been established whether this intracellular form of Aβ is relevant in the neurodegenerative cascade. Despite this cytogeographical difference, Aβ-containing fragments seem to play a critical pathogenic role in IBM. Whereas increased expression of βAPP, aberrant proteolysis, and/or diminished clearance of Aβ-containing fragments in muscle could contribute to amyloid accumulation in IBM muscle fibers, clear evidence exists of excessive βAPP transcripts in IBM (19). Moreover, the subcellular distribution of βAPP seems to be altered in IBM myofibers, away from the postsynaptic domain of the neuromuscular junction to a subsarcolemmal location in IBM fibers (19). Further underscoring the potential pathological consequences of βAPP overexpression in muscle, it has been shown that transfection of normal cultured muscle cells with *βAPP* mRNA leads to IBM-like changes including Congo red-positive amyloid and cytoplasmic tubulofilaments (20, 21).

To test the hypothesis that βAPP mismetabolism is an early component of the molecular pathogenesis of IBM, we derived transgenic mice that selectively overexpress full-length human βAPP in skeletal muscle. These mice develop age-related myopathological and behavioral changes resembling those observed in IBM patients, including intracellular immunoreactivity to Aβ and Aβ-containing fragments, cellular inflammation, and motor deficits. These mice may prove useful for evaluating novel therapeutic interventions and for studying the pathophysiological consequences of intracellular Aβ accumulation outside the central nervous system, which may provide insights into the pathogenesis of AD as well.

Material and Methods

Generation of Transgenic Mice. Human *βAPP* cDNA harboring the Swedish double mutation was subcloned downstream of the 1.3-kb

This paper was submitted directly (Track II) to the PNAS office.

Abbreviations: IBM, inclusion body myositis; AD, Alzheimer's disease; βAPP, amyloid-β precursor protein; Aβ, amyloid-β.

‡To whom reprint requests should be addressed. E-mail: laferla@uci.edu.

The publication costs of this article were defrayed in part by page charge payment. This article must therefore be hereby marked "*advertisement*" in accordance with 18 U.S.C. §1734 solely to indicate this fact.

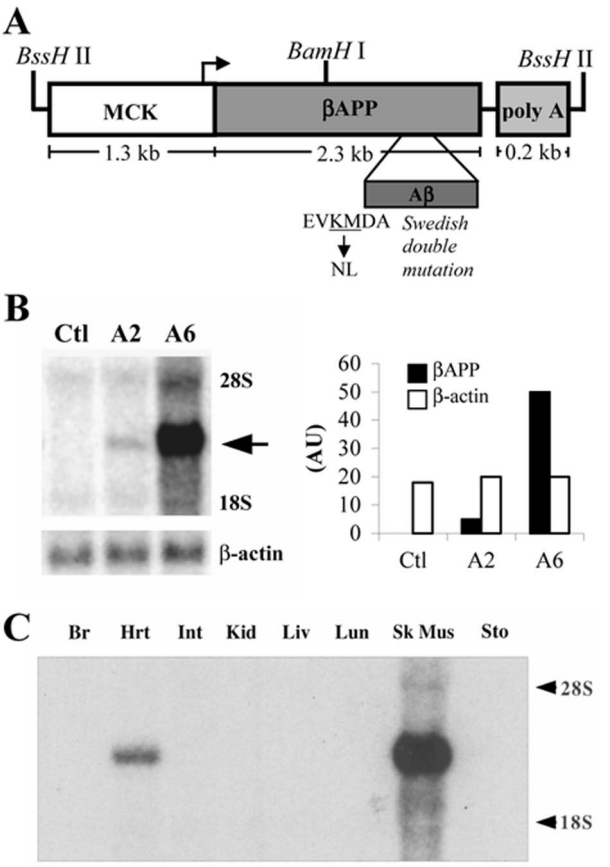

Fig. 1. Transgene map and expression analysis. (*A*) The *MCK* promoter was used to target expression of human *βAPP* cDNA to skeletal muscle. The ≈3.75-kb transgenic construct was isolated by *Bss*HII restriction digestion; also shown is the *Bam*HI site used in the Southern blot analysis. (*B*) Northern blot analysis of skeletal muscle RNA from transgenic mice reveals overexpression of the βAPP transgene in both the A2 and A6 lines. The arrow points to the band corresponding to transgene mRNA. Note that no endogenous βAPP mRNA is detected because the simian virus 40 probe was used. Stripping and reprobing this same blot for β-actin mRNA revealed nearly equivalent RNA loading, indicating that the variation in transgene band intensities accurately reflects differences in transgene expression levels between the two lines. Densitometric analysis reveals approximately 12 times more *βAPP* transgene mRNA in the A6 line than in the A2 line. (*C*) Northern blot analysis of total RNA prepared from several tissues from an A6 mouse (10 weeks of age) shows that expression was selective for muscle with no expression detected in nontarget tissues including brain, intestine, kidney, liver, lung, or stomach. Only muscle expressed the transgene with levels ≈8 times higher in skeletal muscle than in cardiac muscle.

5′ flanking sequence of the *muscle creatine kinase* gene (*MCK*) and upstream of the simian virus 40 polyadenylation signal (Fig. 1*A*). The 3.8-kb transgene was isolated from the cloning vector by digestion with *Bss*HII and purified by sucrose gradient fractionation. After overnight dialysis in injection buffer (10 mM Tris, pH 7.5/0.25 mM EDTA), the construct was microinjected into the pronuclei of single-cell embryos from C57BL6/SJL mice (The Jackson Laboratory) at the University of California, Irvine, Transgenic Mouse Facility. Transgenic mice were identified by Southern blot analysis of tail DNA digested with *Bam*HI (22, 23). The blot was hybridized with a random-primed ^{32}P-labeled probe that encompassed the entire transgene cassette as described (22, 23). Transgenic lines were maintained as hemizygous strains so that nontransgenic control mice were produced in each litter.

Expression Analysis. Hind limb skeletal muscles from 10-week-old transgenic mice were mechanically homogenized, and total RNA was isolated by the guanidinium isothiocyanate-acid phenol method (24). RNA (10 μg) was loaded onto a denaturing agarose/formaldehyde gel and transferred to nitrocellulose. To label transgene mRNA only, Northern blots were hybridized with a random-primed ^{32}P-labeled 0.24-kb simian virus 40 poly(A) DNA fragment. Blots were stripped and reprobed for β-actin mRNA to control for RNA loading. For quantification of band intensities, Phosphorimaging screens (Bio-Rad) were scanned on the Storm system and densitometric analysis was performed with IMAGEQUANT software.

Antibodies. Antibody sources were as follows: anti-Aβ (4G8 and 6E10; Signet Laboratories, Dedham, MA), (anti-$A\beta_{x-40}$ and anti-$A\beta_{x-42}$; BioSource International, Camarillo, CA); anti-actin (Sigma); anti-CD3ε (anti-T-cell; PharMingen); anti-CD11b (anti-macrophage; Sigma); anti-neutrophil (Serotec); anti-βAPP (22C11; Roche Molecular Biochemicals).

Immunoblot Analysis. Skeletal muscle from the hind limb of transgenic mice was mechanically homogenized for 20 sec in buffer containing 2.5% SDS supplemented with a Complete Mini Protease Inhibitor Tablet (Roche). To remove insoluble proteins, homogenized samples were spun at 100,000 × *g* for 60 min at 8°C. For βAPP and β-actin immunoblots, soluble protein extracts were resolved by SDS/PAGE (7.5% Tris-acetate from Invitrogen) under reducing conditions, transferred to nitrocellulose, and probed with monoclonal antibody 6E10 or anti-β-actin at dilutions of 1:500 and 1:1000, respectively. To detect the C99 fragment of βAPP, protein extracts were resolved by using 10% [bis(2-hydroxyethyl)amino] tris(hydroxymethyl)methane SDS/PAGE (Invitrogen) and probed with 6E10. To solubilize any fibrillar Aβ, SDS-insoluble pellets were extracted in 70% formic acid and centrifuged at 100,000 × *g* for 60 min at 8°C.

Immunocytochemical and Histological Analysis of Skeletal Muscle. Formalin-fixed, paraffin-embedded muscle was sectioned at 10 μm and mounted on silane-coated slides and processed as described (22). For cryosections, muscle tissue was frozen in liquid nitrogen-cooled isopentane, sectioned at 10 μm, and stored at −20°C. Primary antibodies were applied at dilutions of 1:1000 for 4G8 and 6E10; 1:500 for anti-$A\beta_{1-40}$ and anti-$A\beta_{1-42}$; 1:100 for anti-neutrophil, anti-CD3ε, and anti-CD11b. Sections were developed with diaminobenzidine substrate by using the avidin-biotin horseradish peroxidase system (Vector Laboratories).

ELISA Measurement. $A\beta_{1-40}$ and $A\beta_{1-42}$ were measured as described by using the BAN50/BA27 and BAN50/BC05 ELISA system (25–28). SDS and formic acid fractions isolated from skeletal muscle as described above were used in the Aβ ELISAs. SDS fractions were diluted 1:40 in buffer (0.1 M NaH_2PO_4/0.1 M Na_2HPO_4/0.05% NaN_3/2 mM EDTA/0.4 M NaCl/1% BSA/0.05% 3-[(3-cholamidopropyl)dimethylammonio]-1-propanesulfonate) (27) and formic acid fractions were diluted 1:20 in 1 M Tris base before loading onto ELISA plates. MaxiSorp immunoplates (Nunc) were coated with BAN50 at a concentration of 5 μg/ml in 0.1 M $NaCO_3$ buffer, 9.6, and blocked with 1% Block Ace (Snow Brand Milk Products, Sapporo, Japan). Synthetic Aβ standards, internal controls, and samples were run at least in duplicate. After overnight incubation at 4°C, wells were probed with either horseradish peroxidase-conjugated BA27 (for $A\beta_{1-40}$) or BC05 (for $A\beta_{1-42}$) for 2–3 h at 37°C. 3,3′,5,5′-tetramethylbenzidine was used as the chromogen, and the reaction was stopped by 6% *O*-phosphoric acid, and read at 450 nm on a Molecular Dynamics plate reader. Numbers of mice used were as follows: nontransgenics, total $n = 11$; A2, $n = 13$; A6, $n = 13$.

Immunodepletion of βAPP and βAPP C-terminal fragments, which includes full-length βAPP, C83 and C99, was performed as follows. SDS-extracted skeletal muscle tissue was diluted 1:20 in RIPA buffer (0.15 mM NaCl/0.05 mM Tris·HCl, pH 7.2/1% Triton

X-100/1% sodium deoxycholate/0.1% SDS) and incubated overnight at 4°C in the presence of 5 μl of CT-20 antiserum (directed against the last 20 aa of βAPP; refs. 26 and 29), and 50 μl of protein A-agarose (GIBCO/BRL). The cleared extract was loaded onto ELISA plates and read against synthetic Aβ standards prepared in the same buffer.

Motor Performance Evaluation. Motor coordination and balance were evaluated with use of the accelerating rotarod apparatus (Acuscan Instruments, Columbus, OH; refs. 30 and 31). Mice were placed on a rotating dowel, and required to continuously walk forward to avoid falling off. The rod accelerated over 20 sec to a constant speed of 20 rpm and the latency to fall was recorded automatically by beams of light that, when broken, stopped a timer. Transgenic mice from the A2 and A6 lines were tested along with nontransgenic littermates. Mice were given 20 training trials, followed by 5 test trials, separated by 1 day between trials.

Results

Transgene Expression Analysis. To test the hypothesis that βAPP mismetabolism plays a causal role in the pathogenesis of IBM, transgenic mice were derived in which human *βAPP* expression was selectively targeted to skeletal muscle by using the mouse *MCK* promoter (Fig. 1*A*). We selected this promoter because in other transgenic models it directed robust expression to muscle, particularly to skeletal as compared with cardiac muscle (32, 33); expression is maintained throughout adulthood (34), an important criterion given that IBM is an age-related disorder. Five transgenic founder mice (referred to as A2, A4, A6, D10, and F9) were identified by Southern blot analysis (data not shown) and were backcrossed to C57/BL6 mice. Three of the five lines (A2, A6, and D10) transmitted the transgene to the F_1 generation.

To assay for transgene expression, we analyzed total RNA from skeletal muscle by Northern blot. To avoid visualizing endogenous mouse *βApp* mRNA, we used a probe targeted to the simian virus 40 polyadenylation region because it was specific for the transgene-produced transcript. We found that the A2 and A6 lines expressed the transgene in muscle to relatively low and high levels, respectively (Fig. 1*B*). Densitometric measurements of Northern blots indicated that the A6 line expressed the transgene approximately 12 times more than the A2 line (Fig. 1*B*). No evidence of transgene expression was found by Northern blot analysis or by reverse transcription–PCR in the D10 line, so it was not characterized further.

Although other transgenic models have achieved overexpression of the carboxy-terminal 99 amino acids of βAPP (C99) in muscle, expression was under the control of a global promoter, and not restricted solely to muscle tissue (35, 36). To determine if *βAPP* transgene expression in the A2 and A6 lines is muscle specific, RNA from a variety of tissues including brain, intestine, kidney, liver, lung, and stomach was analyzed by Northern blot. In both transgenic lines, we found that *MCK*-directed transgene expression was exclusive to skeletal and cardiac muscle, with transgene mRNA levels ≈8 times higher in skeletal muscle than in heart (Fig. 1*C*). Notably, no transgene expression was detected in the nontarget tissues (Fig. 1*C*). These findings are consistent with other transgenic studies that used this same promoter (32, 33).

Steady-state levels of the transgene-derived human protein were determined by Western blot analysis on total protein extracted from skeletal muscle of transgenic mice with an antibody that recognizes human but not murine βAPP. We detected human βAPP in protein extracts of skeletal muscle from both the A2 and A6 lines, with steady-state levels ≈9 times higher in the A6 line than in the A2 line (Fig. 2 *A* and *B*). As expected, we did not detect any human βAPP-immunoreactivity in skeletal muscle extracts from nontransgenic control littermates (Fig. 2*A*).

To compare transgene-derived human βAPP levels in both transgenic lines to endogenous murine βApp levels, Western blot analysis was performed with 22C11, an antibody that recognizes both murine and human βAPP (Fig. 2*C*). The A2 and A6 transgenic lines accumulate ≈3 and 10 times the level of βAPP in skeletal muscle, respectively, when compared with an age-matched nontransgenic mouse (Fig. 2*D*). To determine whether levels of βAPP expression are altered with age, we examined expression levels by Western blot by using the human-specific 6E10 antibody and found that steady-state levels of transgene-derived βAPP remain relatively stable (Fig. 2 *E* and *F*), with a modest decline at 19–21 and 24–26 months of age. These data are consistent with other studies that show that the MCK promoter maintains expression in transgenic mice throughout adulthood (34). The first step in the generation of the Aβ peptide is the endoproteolysis of the βAPP molecule at the β-secretase site to liberate C99. We detected accumulation of the C99 fragment by using 6E10 in skeletal muscle from adult transgenic mice varying in age from 4 to 26 months, although none was detected in age-matched nontransgenic controls (Fig. 2*G*). The steady-state levels of the transgene-derived C99

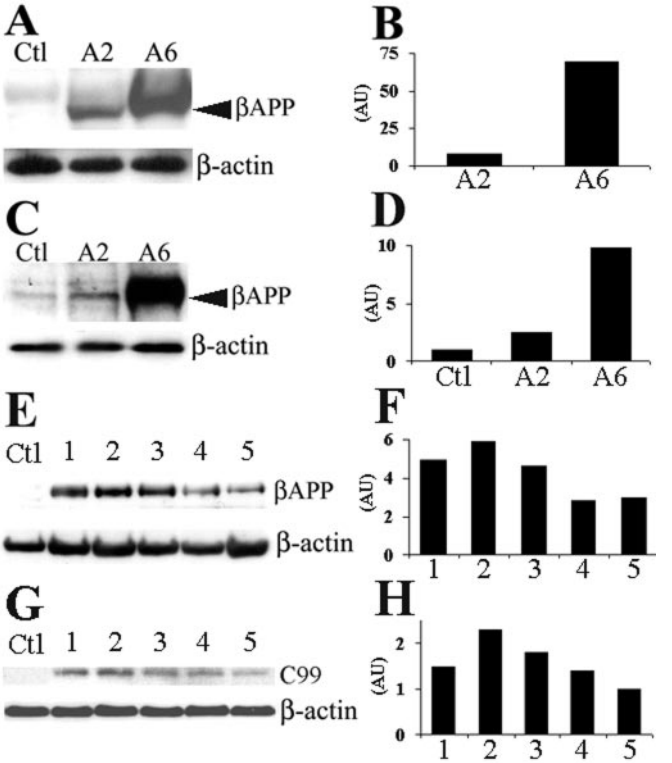

Fig. 2. Immunoblot analysis of βAPP and carboxy-terminal fragments in skeletal muscle. Protein extracts from skeletal muscle were prepared from age-matched transgenic mice from the A2 and A6 lines along with a nontransgenic littermate. Both transgenic lines clearly show accumulation of the human βAPP protein (indicated by the arrowhead) whereas, as expected, no signal was detected in nontransgenic control littermates (referred to as Ctl) when immunoprobed with 6E10 (*A*). To compare transgene-derived βAPP levels with endogenous mouse βApp, skeletal muscle extracts were prepared and immunoprobed with 22C11, which labels both murine and human βAPP (designated by the arrowhead) (*C*). Skeletal muscle from A6 transgenic mice was immunoprobed with human-specific 6E10 to determine the steady-states levels of transgene-derived βAPP as a function of age (*E*). Representative immunoblot using 6E10 that shows steady-state levels of the C99 fragment of βAPP on skeletal muscle extracts from adult A6 transgenic mice of varying ages is shown (*G*). Both βAPP and C99 show fairly stable steady-state levels of the transgene product with a modest decline with advanced age. For *E–H*, lane Ctl = nontransgenic, lane 1 = 4–6 mo, lane 2 = 9–11 mo, lane 3 = 14–16, lane 4 = 19–21 mo, and lane 5 = 24–26; n = 4–5 mice per each time point. Densitometric analysis of band intensities after normalization to β-actin for each corresponding blot are shown in *B*, *D*, *F*, and *H*.

Table 1. Summary of *MCK-βAPP* mice exhibiting IBM-like pathology in skeletal muscle

Pathology	Age, months			
	0–10	10–15	15–20	20–30
Intracellular Aβ immunoreactivity				
A2	0/4	1/3	2/3	2/5
A6	0/4	2/3	1/2	2/2
Inflammation				
A2	0/4	1/3	3/3	2/5
A6	0/4	1/3	1/2	2/2
Centric nuclei				
A2	0/4	0/3	2/3	2/5
A6	0/4	0/3	1/2	2/2

fragment parallel the temporal pattern of the human βAPP holoprotein (compare Fig. 2 *F* and *H*).

IBM-Like Histopathology in *MCK-βAPP* Mice. Skeletal muscle samples from *MCK-βAPP* mice were histologically and immunohistochemically evaluated to determine the pathological consequences of human βAPP overexpression. In muscle from A2 and A6 mice that were less than 10 months of age, we did not detect any overt histopathological alterations. After this time period, however, we noted several IBM-like changes in the transgenic muscle, including centric nuclei, intracellular Aβ immunoreactivity, and cellular inflammation (Table 1). All of these histopathological changes were restricted to focal regions of the muscle tissue, in apposition to histologically normal appearing fibers, consistent with the focal nature of the human disease.

Representative HE-stained sections of skeletal muscle from nontransgenic and transgenic mice are shown (Figs. 3 *A–C*). Note that in the nontransgenic section, the nuclei are peripherally located but that in the transgenic tissue, they are located in the center of the muscle fiber (compare Figs. 3 *A* and *B*). Centric nuclei are a general marker of muscle pathology often observed in muscle disorders, although they can occasionally be found in normal mouse and human tissue at a low frequency (1–3%; ref. 37). The occurrence of centric nuclei in a cluster of myofibers is indicative of underlying cellular damage and subsequent regenerative process in which the centric nuclei arise from newly recruited myoblasts to the site of degeneration. Hence, the occurrence of centric nuclei in focal regions of muscle in aged transgenic mice is consistent with the hypothesis that βAPP mismetabolism can lead to muscle fiber degeneration.

The presence of intramyofibril Aβ is a defining histopathological feature of IBM muscle biopsies and is used, in part, for its diagnosis (39). In skeletal muscle tissue sections from aged (>10 months) mice of both the A2 and A6 lines, we detected Aβ immunoreactivity by using several different Aβ antibodies (Figs. 3 *E–G, I*). As in human IBM, the Aβ immunoreactivity in the transgenic tissue was predominantly, if not exclusively, intracellular. Moreover, in the transgenic tissue, the Aβ immunostaining was not widely distributed throughout the tissue but was present in clusters of muscle

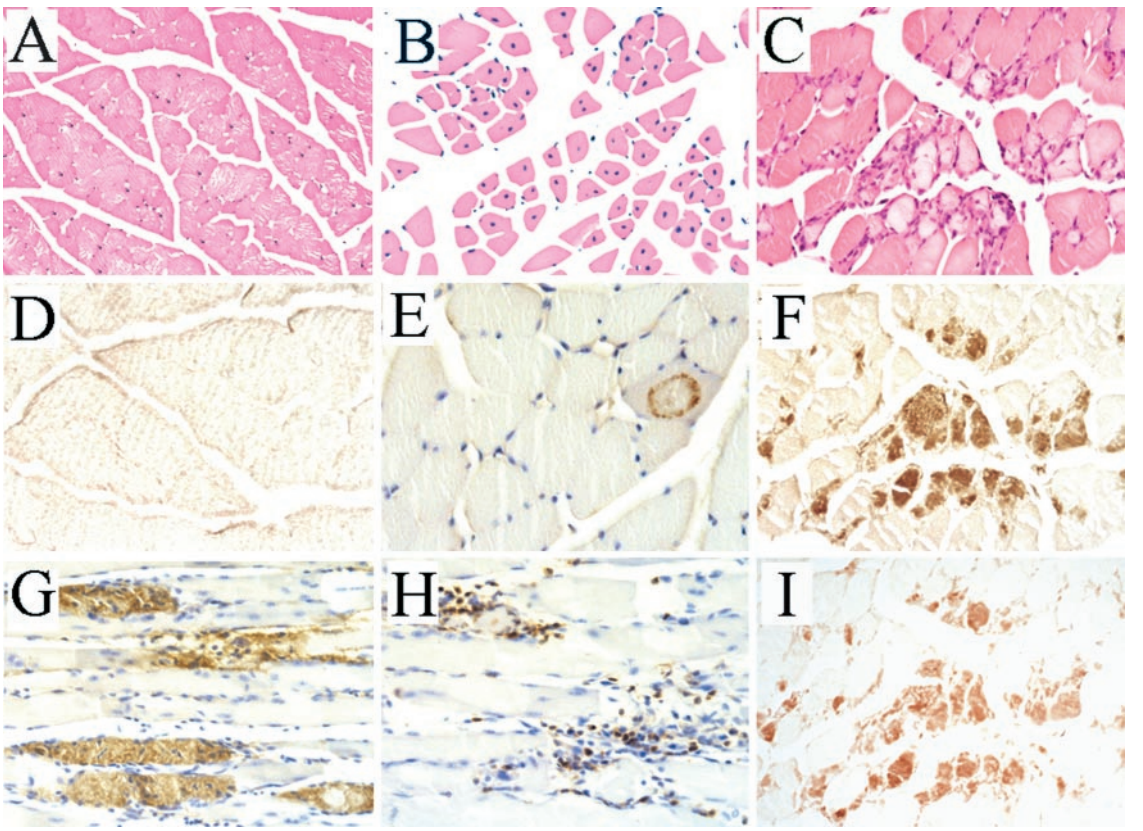

Fig. 3. Myopathological changes in *MCK-βAPP* mice. (*A*) Hematoxylin and eosin (HE) staining of nontransgenic skeletal muscle reveals fibers uniform in size containing peripherally located nuclei. (*B*) Muscle in aged *MCK-βAPP* mice harbor multiple fibers with centric nuclei. (*C*) HE staining of *MCK-βAPP* skeletal muscle reveals variable fiber size and focal regions containing basophilic mononuclear cells that correlates in serial sections with (*F*) intracellular Aβ immunoreactivity. The pattern of intracellular Aβ accumulation occurred as diffuse amorphous deposits and as circular granular patterns (compare *E, F, G,* and *I*) none of which were present in control tissue (*D*). (*H*) Neutrophils were identified as the predominant inflammatory cell type. Skeletal muscle sections of transgenic mice are shown: *B*, A2 line (15 months); *C*, *F, I,* A2 line (16 months); *E*, A2 line (14 months); *G*, A6 line (12 months); *H*, A6 line (14 months). Nontransgenic sections: *A*, 15 months; *D*, 16 months. (Original magnifications: *A*, *B*, ×100; *C–H,* ×400.) Antibodies used: *F, G* (4G8); *E* (6E10); *D* (4G8, 6E10,22C11, $A\beta_{x-40}$, and anti-$A\beta_{x-42}$); *I* (anti-$A\beta_{x-42}$).

fibers in focal regions. The intracellular Aβ immunoreactivity occurred in two distinct forms, as either amorphous diffuse structures (Fig. 3 *F, G,* and *I*) or as punctate granular deposits in ring-like patterns (Fig. 3*E*). It is important to emphasize that a variety of Aβ antibodies were used, including 6E10 and 4G8 and end-specific antibodies. Regardless of the Aβ antibody used, consistent immunoreactivity was observed (compare Fig. 3 *F* and *I*). Despite expression of the transgene in early adulthood, we did not detect any Aβ immunoreactivity in muscle of transgenic mice less than 10 months of age. Likewise, we did not detect any Aβ immunostaining in nontransgenic muscle across all age groups examined (Fig. 3*D*).

The presence of strongly basophilic mononuclear cells was another histopathological change observed in transgenic skeletal muscle. To determine the identity of the infiltrating cell type(s), tissue sections were immunostained with T cell-, macrophage-, and neutrophil-specific antibodies. We did not detect immunostaining with either the T cell- or macrophage-specific antibodies. In contrast, prominent neutrophil-specific immunoreactivity was evident in the transgenic tissue (Fig. 3*H*). The occurrence of inflammation represents an important component of our model, because it is a defining pathological characteristic of sporadic, but not hereditary IBM (38). In sporadic IBM, T cell inflammation represents the major inflammatory cell type, but in our mouse model, neutrophils were the predominant cell type; the relevance of this disparity is presently unclear, but may be related to the expression of the transgene throughout ontogeny. A strong overlap exists between regions showing immune infiltration and Aβ immunoreactivity as shown in serial sections (compare Fig. 3 *C* and *F*). Nevertheless, we could also detect intracellular Aβ immunoreactivity in regions without any prominent inflammation, consistent with the notion that accumulation of Aβ-containing fragments represents an early pathogenic event followed by immune infiltration (data not shown).

ELISA Measurements. βAPP overexpression in muscle leads to development of IBM-like muscle pathology, which might be caused by one of its various proteolytic derivatives. Levels of these βAPP proteolytic fragments were quantified by using a well-characterized and highly sensitive ELISA system that can distinguish between steady-state levels of $A\beta_{40}$ and $A\beta_{42}$ (25–28, 40, 41). Levels of $A\beta_{42}$ in the nontransgenic muscle samples were relatively low, ranging from 0.1 to 1.4 fmol/mg. Likewise, in the low expressing A2 transgenic line, $A\beta_{42}$ levels were marginally higher than age-matched nontransgenic controls, ranging from 0.3 to 3.1 fmol/mg. In the high expressing A6 line, however, $A\beta_{42}$ levels were markedly higher across all ages than both the A2 line and nontransgenic controls, ranging from 6.0 to 16.2 fmol/mg. No $A\beta_{40}$ or $A\beta_{42}$ signal was detectable in formic acid fractions from either the A2 or A6 transgenic line (data not shown).

Because the Aβ antibodies used in the ELISAs can crossreact with Aβ-containing fragments such as C99, we sought biochemical confirmation to determine the precise source of the Aβ signal observed. To assess this possibility, we immunodepleted the SDS-extracted skeletal muscle tissue with an antibody directed against the last 20 aa of βAPP. This antibody will efficiently immunoprecipitate either full-length βAPP or any βAPP fragments that contain these residues, including C83 and C99. SDS extracts "cleared" in this manner demonstrated markedly reduced ($85 \pm 7\%$; $n = 10$) $A\beta_{42}$ readings. These findings indicate that there is a small amount of Aβ in these samples but that the predominant Aβ-containing fragment that appears to accumulate in the transgenic muscle is C99. Moreover, these findings along with the observation that no Aβ was detected in the formic acid fraction may explain why we failed to detect any congophilic-positive staining.

MCK-βAPP Mice Exhibit an Age-Related Deficit in Rotarod Performance. Transgenic mice did not display any overt behavioral abnormalities nor was their life span diminished compared with nontransgenic control littermates. Because muscle weakness is the primary clinical component of IBM, we investigated whether deficits in muscle balance and coordination accompanied the underlying histopathological changes in *MCK-βAPP* muscle. Mice were evaluated on the accelerating rotarod, a well characterized behavioral task designed to assess motor performance (30, 31). At the earlier times (<10 months of age) we did not detect significant differences in performance between transgenic and nontransgenic mice (Fig. 4). In both the A2 and A6 lines, we noticed diminished performance between transgenic mice and age-matched controls beginning at 10–15 months of age. For the A6 line, these differences were statistically significant ($P < 0.05$, Student's t test) in mice beginning at 15–20 months of age when compared with nontransgenic control mice. Although transgenic mice from the A2 line displayed a similar trend toward an age-related decrease in their ability to remain on the rotarod compared with nontransgenic mice, these differences were not statistically significant. The relative differences in motor performance correlate with the low and high transgene expression levels observed between A2 and A6 lines.

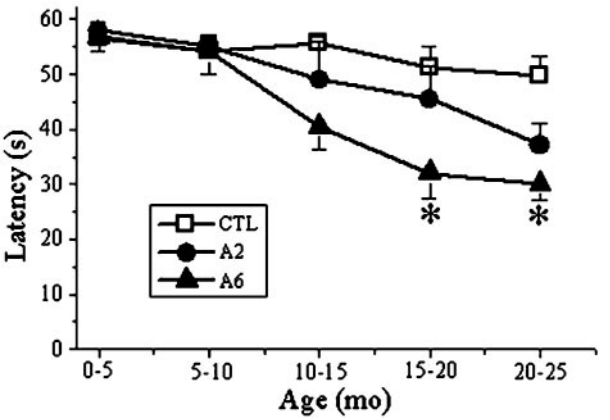

Fig. 4. *MCK-βAPP* mice display an age-related decrease in motor performance on the accelerating rotarod. As *MCK-βAPP* mice age, their ability to remain on the rotarod diminishes compared with age-matched nontransgenic littermates. These differences were significant for aged transgenic mice in the A6 line compared with controls at 15–20 and 20–25 months of age ($P < 0.05$, Student's t test). Transgenic mice from the A2 line display a trend toward an age-related decline in motor performance as well, although these data were not statistically significant. Error bars represent the SEM. Mice between 26 and 34 g were used in the analyses. Numbers of mice evaluated were as follows: A2 and [A6] transgenic mice 0–5 months $n = 6$ (6); 5–10 months $n = 6$ (6); 10–15 months $n = 4$ (5); 15–20 months $n = 4$ (6); 20–25 months $n = 9$ (8). Age-matched nontransgenic littermates were used as controls: 0–5 months $n = 6$; 5–10 months $n = 6$; 10–15 months $n = 6$; 15–20 months $n = 6$; 20–25 months $n = 8$.

Discussion

Here we derived two independent transgenic lines that selectively overexpress human βAPP in skeletal muscle. Both *MCK-βAPP* transgenic lines consistently developed a subset of IBM-like pathological changes in an age-dependent fashion that included increased formation of Aβ-containing βAPP proteolytic fragments and a neutrophil-mediated inflammatory response that was clustered around βAPP immunoreactive regions. In addition, βAPP overexpression in muscle leads to age-related deficits in motor performance.

Despite differing transgene expression levels between A2 and A6 mice, both lines develop comparable myopathology, which may be because tissue pathology is a dynamic process and may be subject to ongoing clearance. Continual clearance would account for the comparable pathology between the two lines despite the disparity in transgene expression. The occurrence of centric nuclei in the A2 and A6 transgenic myofibers supports this supposition (Fig. 3*B*), as it likely reflects newly recruited myoblasts to the sites of degener-

ation. It is critical to emphasize that the behavioral phenotype, however, strongly correlates with transgene expression levels, as the A6 line exhibits an earlier and more severe decline in motor performance on the rotarod compared with the A2 line.

Although the etiology underlying sporadic IBM is not yet known, these data and those of others (35, 36) provide additional *in vivo* evidence implicating βAPP mismetabolism as an early, upstream event in the molecular pathogenesis of human IBM. In addition to Aβ deposition, the intracellular accumulation of C- and N-terminal βAPP epitopes has been documented immunohistochemically in IBM muscle (42), and the accumulation of other βAPP proteolytic fragments has been documented by Western blotting (43).

IBM-like histopathological changes were observed in transgenic mice older than 10 months of age, but not in younger transgenic or nontransgenic mice, mirroring the age-related aspect of human IBM. The motor deficits were also manifested as a function of age in our transgenic lines with the greatest decline occurring in the high expressing A6 line. Because the *MCK* promoter is transcriptionally active in young mice (34 and Fig. 2 *E* and *F*), it suggests that other unknown age-related factors are required for the elaboration of these phenotypic changes (Fig. 4). Despite expression of the transgene in every A2 or A6 mouse analyzed, not all aged transgenic mice developed intracellular Aβ immunoreactive deposits or other myopathological changes such as centric nuclei and atrophic fibers (Table 1). Although we have no clear explanation for the incomplete penetrance, these results are consistent with studies showing that only a portion of transgenic mice that globally overexpressed the C100 fragment of βAPP, exhibited intramyofibril Aβ deposits (35, 36). Nevertheless, we believe the phenotype we describe is directly due to overexpression of βAPP for the following reasons: (*i*) comparable pathology to that described here has not been reported in other mouse models using the same MCK promoter; (*ii*) we demonstrate a similar behavioral and myopathological phenotype in two independent lines, arguing against nonspecific effects caused by integration of the transgene; and (*iii*) the higher expressing A6 line shows a more dramatic deficit in rotarod performance compared with the lower expressing A2 line.

This transgenic model enables us to understand better the process by which accumulation of amyloidogenic fragments lead to cellular degeneration. In particular, because βAPP mismetabolism is involved in the pathogenesis of both AD and IBM, insights learned about one disorder may also be applicable to the other. An interesting distinction between the two disorders relates to the cellular location of the Aβ peptide, which is predominantly intracellular in IBM. Nevertheless, accumulating evidence suggests that intracellular Aβ may be an important and underappreciated component of AD pathology (17, 18, 44–46). Finally, given that no effective treatments exist for IBM patients, this mouse model offers the potential for evaluating the efficacy of novel therapeutics.

We thank Drs. Rachel Neve and Stephen Hauschka for kindly providing the *βAPP* cDNA and *MCK* promoter DNA sequence, Vincent Caiozzo and Aileen Anderson for technical advice and expertise, and Mr. Tom Fielder for microinjection of the transgene. This study was supported by Grants AG15409 and AG00096 from the National Institute on Aging.

1. Selkoe, D. J. (2001) *Physiol. Rev.* **81,** 741–766.
2. Dalakas, M. C. (1992) *Clin. Neuropharmacol.* **15,** 327–351.
3. Oldfors, A. & Lindberg, C. (1999) *Curr. Opin. Neurol.* **12,** 527–533.
4. Askanas, V. & Engel, W. K. (1993) *Curr. Opin. Rheumatol.* **5,** 732–741.
5. Yunis, E. J. & Samaha, F. J. (1971) *Lab. Invest.* **25,** 240–248.
6. Amato, A. A. & Barohn, R. J. (1997) *Neurol. Clin.* **15,** 615–648.
7. Askanas, V., Engel, W. K., Mirabella, M., Weisgraber, K. H., Saunders, A. M., Roses, A. D. & McFerrin, J. (1996) *Ann. Neurol.* **40,** 264–265.
8. Harrington, C. R., Anderson, J. R. & Chan, K. K. (1995) *Neurosci. Lett.* **183,** 35–38.
9. Askanas, V., Engel, W. K., Bilak, M., Alvarez, R. B. & Selkoe, D. J. (1994) *Am. J. Pathol.* **144,** 177–187.
10. Askanas, V., Bilak, M., Engel, W. K., Alvarez, R. B., Tome, F. & Leclerc, A. (1993) *NeuroReport* **5,** 25–28.
11. Askanas, V., Mirabella, M., Engel, W. K., Alvarez, R. B. & Weisgraber, K. H. (1994) *Lancet* **343,** 364–365.
12. Askanas, V., Engel, W. K., Yang, C. C., Alvarez, R. B., Lee, V. M. & Wisniewski, T. (1998) *Am. J. Pathol.* **152,** 889–895.
13. Askanas, V., Engel, W. K., Alvarez, R. B., McFerrin, J. & Broccolini, A. (2000) *J. Neuropathol. Exp. Neurol.* **59,** 592–598.
14. Kuo, Y. M., Kokjohn, T. A., Watson, M. D., Woods, A. S., Cotter, R. J., Sue, L. I., Kalback, W. M., Emmerling, M. R., Beach, T. G. & Roher, A. E. (2000) *Am. J. Pathol.* **156,** 797–805.
15. Fandrich, M., Fletcher, M. A. & Dobson, C. M. (2001) *Nature (London)* **410,** 165–166.
16. Askanas, V., Engel, W. K. & Alvarez, R. B. (1992) *Am. J. Pathol.* **141,** 31–36.
17. LaFerla, F. M., Troncoso, J. C., Strickland, D. K., Kawas, C. H. & Jay, G. (1997) *J. Clin. Invest.* **100,** 310–320.
18. Gouras, G. K., Tsai, J., Naslund, J., Vincent, B., Edgar, M., Checler, F., Greenfield, J. P., Haroutunian, V., Buxbaum, J. D., Xu, H., *et al.* (2000) *Am. J. Pathol.* **156,** 15–20.
19. Sarkozi, E., Askanas, V., Johnson, S. A., Engel, W. K. & Alvarez, R. B. (1993) *NeuroReport* **4,** 815–818.
20. Askanas, V., McFerrin, J., Baque, S., Alvarez, R. B., Sarkozi, E. & Engel, W. K. (1996) *Proc. Natl. Acad. Sci. USA* **93,** 1314–1319.
21. Askanas, V., McFerrin, J., Alvarez, R. B., Baque, S. & Engel, W. K. (1997) *NeuroReport* **8,** 2155–2158.
22. LaFerla, F. M., Tinkle, B. T., Bieberich, C. J., Haudenschild, C. C. & Jay, G. (1995) *Nat. Genet.* **9,** 21–30.
23. LaFerla, F. M., Sugarman, M. C., Lane, T. E. & Leissring, M. A. (2000) *J. Mol. Neurosci.* **15,** 45–59.
24. Chomczynski, P. & Sacchi, N. (1987) *Anal. Biochem.* **162,** 156–159.
25. Murphy, M. P., Hickman, L. J., Eckman, C. B., Uljon, S. N., Wang, R. & Golde, T. E. (1999) *J. Biol. Chem.* **274,** 11914–11923.
26. Murphy, M. P., Uljon, S. N., Fraser, P. E., Fauq, A., Lookingbill, H. A., Findlay, K. A., Smith, T. E., Lewis, P. A., McLendon, D. C., Wang, R. & Golde, T. E. (2000) *J. Biol. Chem.* **275,** 26277–26284.
27. Suzuki, N., Cheung, T. T., Cai, X. D., Odaka, A., Otvos, L., Eckman, C., Golde, T. E. & Younkin, S. G. (1994) *Science* **264,** 1336–1340.
28. Kuo, Y. M., Emmerling, M. R., Vigo-Pelfrey, C., Kasunic, T. C., Kirkpatrick, J. B., Murdoch, G. H., Ball, M. J. & Roher, A. E. (1996) *J. Biol. Chem.* **271,** 4077–4081.
29. Pinnix, I., Musunuru, U., Tun, H., Sridharan, A., Golde, T., Eckman, C., Ziani-Cherif, C., Onstead, L. & Sambamurti, K. (2001) *J. Biol. Chem.* **276,** 481–487.
30. Jones, B. J. & Roberts, D. J. (1968) *J. Pharm. Pharmacol.* **20,** 302–304.
31. Sango, K., McDonald, M. P., Crawley, J. N., Mack, M. L., Tifft, C. J., Skop, E., Starr, C. M., Hoffmann, A., Sandhoff, K., Suzuki, K. & Proia, R. L. (1996) *Nat. Genet.* **14,** 348–352.
32. Johnson, J. E., Wold, B. J. & Hauschka, S. D. (1989) *Mol. Cell. Biol.* **9,** 3393–3399.
33. Shield, M. A., Haugen, H. S., Clegg, C. H. & Hauschka, S. D. (1996) *Mol. Cell. Biol.* **16,** 5058–5068.
34. Lyons, G., Muhlebach, S., Moser, A., Masood, R., Paterson, B. M., Buckingham, M. E. & Perriard, J. C. (1991) *Development (Cambridge, U.K.)* **113,** 1017–1029.
35. Fukuchi, K., Pham, D., Hart, M., Li, L. & Lindsey, J. R. (1998) *Am. J. Pathol.* **153,** 1687–1693.
36. Jin, L. W., Hearn, M. G., Ogburn, C. E., Dang, N., Nochlin, D., Ladiges, W. C. & Martin, G. M. (1998) *Am. J. Pathol.* **153,** 1679–1686.
37. Adams, J. H. & Duchen, L. W. (1992) *Greenfield's Neuropathology* (Oxford Univ. Press, New York).
38. Askanas, V., Serratrice, G. & Engel, W. K. (1998) *Inclusion-Body Myositis and Myopathies* (Cambridge Univ. Press, Cambridge, U.K.).
39. Askanas, V. & Engel, W. K. (1998) *Curr. Opin. Rheumatol.* **10,** 530–542.
40. Scheuner, D., Eckman, C., Jensen, M., Song, X., Citron, M., Suzuki, N., Bird, T. D., Hardy, J., Hutton, M., Kukull, W., *et al.* (1996) *Nat. Med.* **2,** 864–870.
41. Lue, L. F., Kuo, Y. M., Roher, A. E., Brachova, L., Shen, Y., Sue, L., Beach, T., Kurth, J. H., Rydel, R. E. & Rogers, J. (1999) *Am. J. Pathol.* **155,** 853–862.
42. Askanas, V., Alvarez, R. B. & Engel, W. K. (1993) *Ann. Neurol.* **34,** 551–560.
43. Choi, Y. C., Park, G. T., Kim, T. S., Sunwoo, I. N., Steinert, P. M. & Kim, S. Y. (2000) *J. Biol. Chem.* **275,** 8703–8710.
44. Tienari, P. J., Ida, N., Ikonen, E., Simons, M., Weidemann, A., Multhaup, G., Masters, C. L., Dotti, C. G. & Beyreuther, K. (1997) *Proc. Natl. Acad. Sci. USA* **94,** 4125–4130.
45. Skovronsky, D. M., Doms, R. W. & Lee, V. M. (1998) *J. Cell Biol.* **141,** 1031–1039.
46. Yang, A. J., Chandswangbhuvana, D., Shu, T., Henschen, A. & Glabe, C. G. (1999) *J. Biol. Chem.* **274,** 20650–20656.